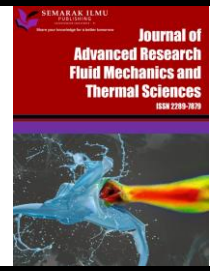




## Journal of Advanced Research in Fluid Mechanics and Thermal Sciences

Journal homepage:  
[https://semarakilmu.com.my/journals/index.php/fluid\\_mechanics\\_thermal\\_sciences/index](https://semarakilmu.com.my/journals/index.php/fluid_mechanics_thermal_sciences/index)  
ISSN: 2289-7879



# Effect of Titanium Dioxide on Cure Characteristics and Physico Mechanical Properties of High-Temperature Vulcanizing Silicone Rubber Composites

Leong Zhi Wei<sup>1</sup>, Noraiham Mohamad<sup>1,\*</sup>, Siti Nor Rohimah Fauzi<sup>1</sup>, Hairul Effendy Ab Maulod<sup>1</sup>, Jeefferie Abd Razak<sup>1</sup>, Soh Tiak Chuan<sup>2</sup>, Qumrul Ahsan<sup>3</sup>

<sup>1</sup> Faculty of Industrial and Manufacturing Technology and Engineering, Universiti Teknikal Malaysia Melaka, Hang Tuah Jaya, 76100, Durian Tunggal, Melaka, Malaysia

<sup>2</sup> JB 748, Lot 41&42, Kawasan Perindustrian Serkam, Merlimau, 77300 Daerah Jasin, Melaka, Malaysia

<sup>3</sup> University of Asia Pacific, 74/A, Green Road, Farmgate, Dhaka-1205, Bangladesh

### ARTICLE INFO

#### Article history:

Received 22 December 2023

Received in revised form 25 April 2024

Accepted 6 May 2024

Available online 30 May 2024

#### Keywords:

Silicone rubber composites; titanium dioxide; cure characteristics; mechanical properties

### ABSTRACT

Silicone rubber (SiR), a vital elastomer, is extensively used in producing various engineering and general products, owing to its distinctive properties. Despite the remarkable properties, SiR-based products require anti-microbial agents such as titanium dioxide, TiO<sub>2</sub> to negate black mold issues. Still, adding this agent alters the composites' processability and physical and mechanical properties. This study examined the impact of adding different TiO<sub>2</sub> content as fillers on silicone rubber composites' processability, physical properties, and mechanical properties. Raw materials of 20-hardness high-temperature-vulcanization (HTV) SiR- reinforced with various TiO<sub>2</sub> contents at 0.0, 0.3, 0.6 and 1.2 wt% were prepared using a two-roll mill. The results indicated SiR composites reinforced with 0.3 wt% TiO<sub>2</sub> exhibited the best performance with a tensile strength of 1.49 MPa, elongation at break of 340.87%, modulus 100% of 0.664 MPa, modulus 300% of 0.822 MPa, and modulus 500% of 0.954 MPa. This performance can be attributed to the efficient crosslink density and the effective interactions between the TiO<sub>2</sub> and silicone rubber particles at this concentration. Structural and morphological analyses further corroborated the results. Consequently, it can be inferred that silicone rubber reinforced with 0.3 wt% titanium dioxide holds the potential for formulating silicone rubber compounds that necessitate anti-microbial properties.

## 1. Introduction

Silicone rubber is an important elastomer for manufacturing various products, such as sealants, swimming caps and baby mats. Silicone rubber is a kind of polymer with elastic (flexible) properties and is also referred to as elastomer. The structure of elastomers is loosely crosslinked and randomly coiled. Alarifi [1] states that elastomers can be stretched or elongated at room temperature. Thus, when the elastomers have been stretched, they could recoil due to crosslinking of the chains. However, the disadvantage is the microbial contamination that causes black molds on silicone

\* Corresponding author.

E-mail address: [noraiham@utem.edu.my](mailto:noraiham@utem.edu.my)

<https://doi.org/10.37934/arfmts.117.2.4659>

rubber, an unavoidable engineering problem [2]. The black molds occur due to microorganisms utilizing silicone rubber as their food source due to exposure to UV and heat in the environment [3]. Figure 1 shows an example of black mold grown on sealant and rubber gasket, which can be noticeable in areas mostly in contact with water. It is unsightly, reduces the sealant's performance and could incur health risks. Therefore research on the aging and degradation of silicone rubber under ultraviolet (UV) irradiation, heat, and chemicals also became a hot topic since it lowers the mechanical properties [3,4]. Researchers and developers have recently focused on improving silicone rubber's mechanical properties, cure characteristics and anti-microbial functions by reinforcing it with titanium dioxide ( $\text{TiO}_2$ ).

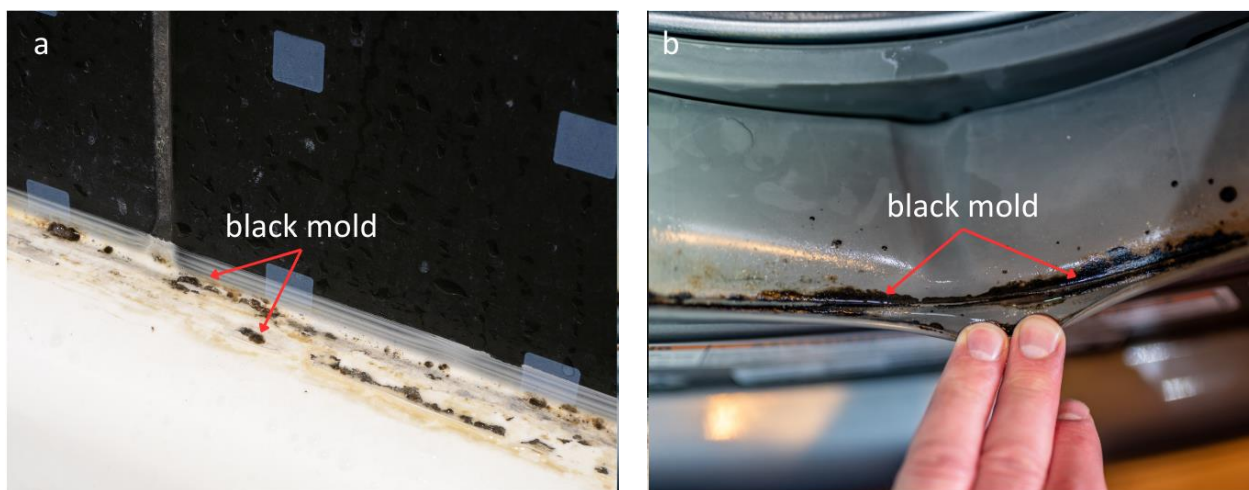


**Fig. 1.** Sample of black mold grown on silicone rubber (a) tiles sealant and (b) washing machine gasket

The siloxane functional group ( $\text{Si-O-Si}$ ) is used in the backbone of silicone rubbers, which are the most frequent inorganic elastomers [5]. Some researchers used zinc oxide mixtures with silicone rubber and tested their antibacterial and mechanical properties for medical applications, successfully finding the best ratio [6]. Numerous studies have included  $\text{TiO}_2$  in polymer matrix composites [7]. As mentioned in a study by Datta *et al.*, [7] investigated the enhancement of natural rubber composites by modifying rutile- $\text{TiO}_2$  nanoparticles and microparticles. The authors demonstrated that adding 5 parts per hundred rubber (phr) of nano- $\text{TiO}_2$  improved mechanical properties. However, a higher concentration of nano- $\text{TiO}_2$  particles resulted in a decrease in these properties. The study also revealed that the composites containing 5 phr of micro- $\text{TiO}_2$  exhibited lower mechanical properties than those with nano- $\text{TiO}_2$ . Sim *et al.*, [8] claim that for silicone rubber compounds filled with alumina ( $\text{Al}_2\text{O}_3$ ), the time it takes to reach a certain level of curing ( $T_{90}$ ) decreases as the filler loading increases, indicating an increment in the cure rate. On the other hand, for silicone rubber compounds filled with ZnO, the  $T_{90}$  decreases with increasing loading up to 10 phr, but beyond that point, the  $T_{90}$  increases with further increases in ZnO loading. Lastly, Wu *et al.*, [9] also claimed that increasing and decreasing tear strength and hardness patterns imply a competition between the elastomer's ongoing crosslinking process and the decomposition of the macromolecule chains.

In a nutshell,  $\text{TiO}_2$ 's presence imposed a critical effect on the mechanical properties of composites. This study would embark on a similar scope except on a different type of matrix, 20-hardness HTV silicone rubber. Moreover, studying the effects of  $\text{TiO}_2$  on the cure characteristics and mechanical properties of 20-hardness HTV silicone rubber is yet to be explored, which is crucial to do the research. In this study, the effect of  $\text{TiO}_2$  on the processability and mechanical properties of 20-hardness HTV silicone rubber will be investigated to motivate improvements in their mechanical and curing properties and to extend the lifetime of silicone rubber products.

## 2. Methodology

### 2.1 Raw Materials and Preparation

The main raw materials involved were 20-hardness HTV silicone rubber, titanium dioxide, and  $\text{TiO}_2$  powder. The general formulations of these materials are tabulated in Table 1, and the compounds are depicted in Figure 2. The masterbatch was a pre-dispersing approach to improve the dispersion of  $\text{TiO}_2$  particles in the compound. It was supplied by Rubber Leisure Products Sdn Bhd (RLPSB). The RLPSB performed the compounding process through a two-roll mill and supplied the composite compounds: 1) the silicone rubber composite (SiR) and 2) the silicon rubber reinforced with titanium dioxide composite (SiR- $\text{TiO}_2$ ) with various contents that were used in this project.

**Table 1**

The formulation for the preparation of silicone rubber reinforced different percentages of titanium dioxide

Sample	1	2	3	4
20-hardness silicone rubber (g)	300.00	200.00	200.00	200.00
Peroxide catalyst (g)	2.25	1.50	1.50	1.50
10% $\text{TiO}_2$ Masterbatch (g)	-	6	12	18
Titanium dioxide, $\text{TiO}_2$ (wt%)	0	0.3	0.6	1.2

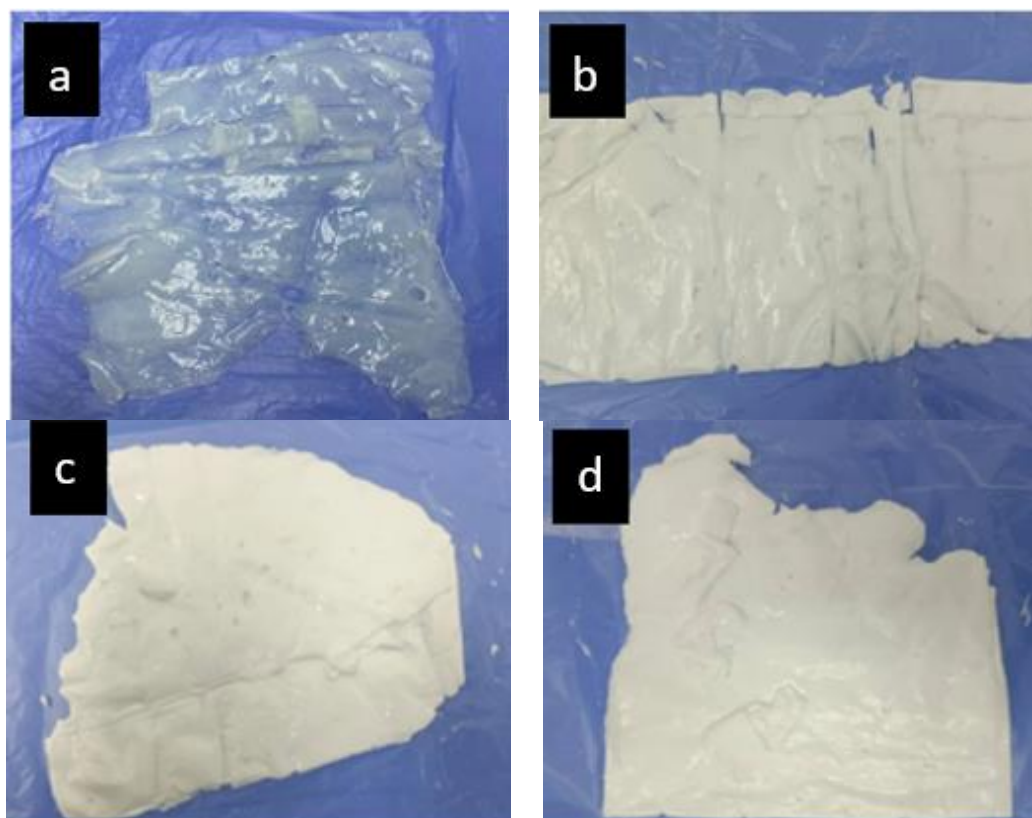


**Fig. 2.** The compounds at various titanium dioxide loadings of (a) 0.0 wt%, (b) 0.3 wt%, (c) 0.6 wt%, and (d) 1.2 wt%

Figure 3 shows the flow of methodology involved in the study. The compounds received from RLPSB were fabricated and simultaneously vulcanized using a hot press machine at FTKIP, UTeM. First, the SiR with SiR- $\text{TiO}_2$  composite compounds was weighed for the hot press process. Then, the desired weighed compound was filled into a mold with a 3 mm thickness. The silicone rubber was

vulcanized simultaneously at 180°C and pressure of 150 kg/force according to the respective cure time,  $T_{90}$ , measured from the cure characteristic test. Then, samples were cut after hot pressing.

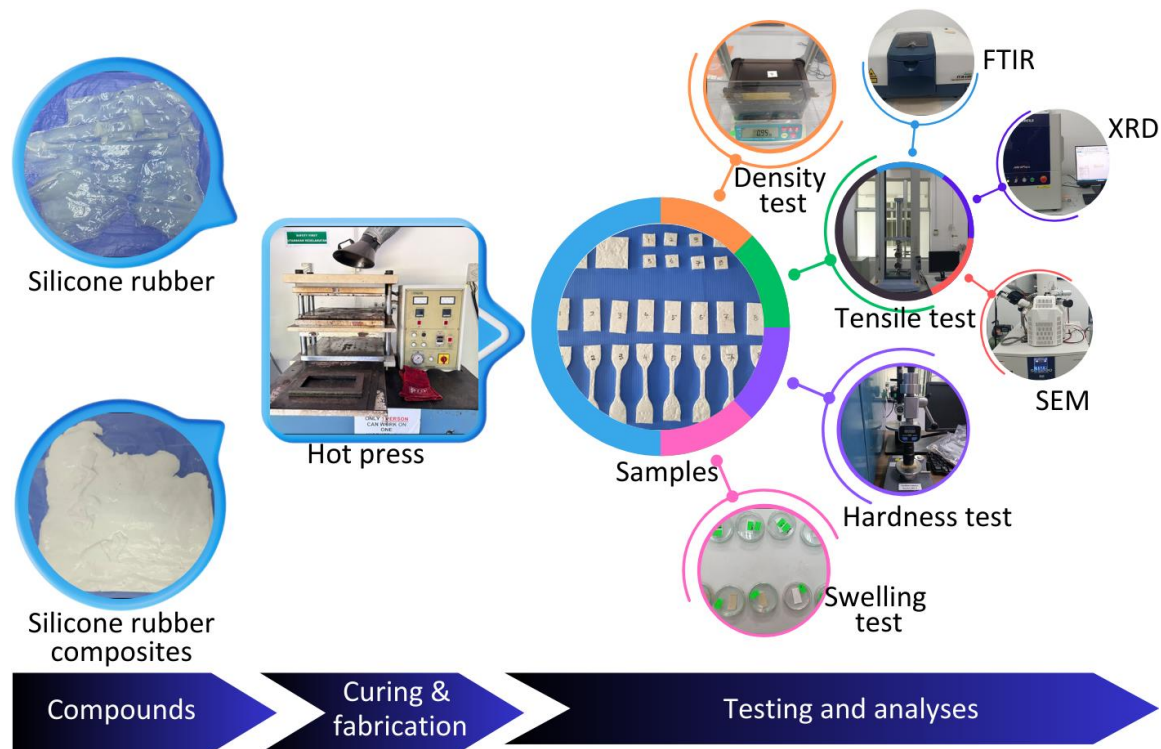


**Fig. 3.** The flow of methodology involved in the study that starts with silicone rubber compounds to hot pressing followed by testing and analysis steps

## 2.2 Testing and Characterizations

### 2.2.1 Cure characteristic, physical testing and swell measurement

The curing characteristics of the silicone rubber composite were obtained by using a U-CAN DYNATEX INC moving die rheometer (UR-2010), which was used to determine torque, scorch time ( $T_{s2}$ ), cure time ( $T_{90}$ ) and cure rate index (CRI) according to ASTM D5289. There were 4 grams of the respective compound samples tested at the vulcanization temperature of 175°C. The cure time was 4 minutes, and the pressure was 5 kg/cm<sup>2</sup>.

The density of composites was measured per ASTM D792 using an electronic densimeter MD-300S (Alfa Mirage, Japan). The average value of at least three measurements was taken for each sample. The samples' hardness (Shore A) was measured by a Shore A tester (Durometer Hardness Meter Bareiss HPE II) according to the ASTM D2240. After repeated measurements for one sample, the median hardness was recorded.

The swell measurement was carried out according to ASTM D471. The cured specimens with dimensions 50mm x 25mm x 2mm were weighed using an electric balance, followed by immersion of toluene for 24 hours at room temperature (25 °C) in a dark environment. After the conditioning period, the swollen specimens were taken out and weighed again to determine the swelling percentage using Eq. (1). Then, the specimens were dried in an oven at 60 °C until a constant weight was reached and the toluene uptake was determined using Eq. (2). The symbols are  $W_0$  = initial mass before immersion (g),  $W_1$  = mass after the swelling (g),  $W_2$  = mass after oven-dried until constant weight (g), and  $W_t$  = molecular weight of toluene (92.14 g/mol).

$$\text{Swelling Percentage (\%)} = \frac{W_1 - W_0}{W_0} \times 100\% \quad (1)$$

$$\text{Toluene Uptake (\%)} = \frac{W_1 - W_2}{W_0} \times 100 / W_t \quad (2)$$

### 2.2.2 Tensile test

Tensile tests were performed at room temperature at 500 mm/min cross-head speed using a Universal Testing Machine (Shimadzu AGS-X Series). It was to determine the tensile properties such as the tensile strength (TS), the modulus at 100% (M100) and 300% (M300) elongations and the elongation at break (EB). The dumbbell specimen shape was according to ASTM D412 Type C.

### 2.2.3 Characterization analyses

The compositional analysis was conducted using the FTIR JASCO FTIR-6100 model X-ray Diffraction (XRD) Analysis. The spectra were generated at room temperature and a 500-4000  $\text{cm}^{-1}$  scanning range. Each spectrum was acquired with 64 scans. Then, the compound sheets were characterized by X-ray diffraction spectroscopy (XRD) using the Rigaku Mini Flex model. XRD spectra of the samples were collected over the  $2\theta$  range of 1 to  $40^\circ$  using copper  $K\alpha$  radiation at a generator voltage of 40 kV, a generator current of 20.0 mA, wavelength,  $\lambda$  of 1.5406 and a step scan rate of  $10^\circ$  in  $2\theta \text{ min}^{-1}$ .

Scanning electron microscopy (SEM) model Hitachi SU8000 was used to identify the morphology of the silicone rubber composites. The morphological inspection on their fracture surface was conducted at 1000X magnifications and 10kV accelerating voltage.

## 3. Results and Discussion

### 3.1 Cure Characteristics and Physical Properties

Table 2 tabulates the cure characteristics, hardness and density of the composites. The scorch time,  $T_{s2}$  denotes the duration a rubber compound can process at a specified temperature before curing [10]. This experiment achieved the highest scorch time at 0.3 wt% titanium dioxide. It can be seen that the presence of filler at 0.3 wt% titanium dioxide reinforced SiR manifested the safest amount of time for the compound to fill up mold during processing compared to compounds at 0.0, 0.6 and 1.2 wt% of  $\text{TiO}_2$ .

**Table 2**  
 Cure characteristics of the composites based on the percentage of titanium dioxide

Cure characteristics	Titanium dioxide (wt%)				Standard deviation ( $\pm$ )
	0.0	0.3	0.6	1.2	
Scorch time (min.sec)	0.54	1.01	0.55	0.57	0.009
Cure time (min.sec)	1.23	1.33	1.28	1.29	0.023
Cure rate index (CRI)	145	313	137	139	-
Minimum torque (dNM)	6.76	7.44	7.93	8.44	0.375
Maximum torque (dNM)	14.83	15.04	15.83	16.79	0.263
Torque difference (dNM)	8.07	7.6	7.9	8.35	-
Hardness (Shore A)	18.92	19.68	20.76	16.12	0.481
Density ( $\text{g/cm}^3$ )	1.054	1.022	1.070	0.812	0.026

The shorter scorch time indicated the sample was easily cured, which is not good for processability. Thus, it was found that there were further decreases in the scorch time when SiR reinforced 0.6 and 1.2 wt% titanium dioxide. Excessive TiO<sub>2</sub> added in SiR had a greater effect on reducing the scorch time. Chueangchayaphan *et al.*, [11] indicated that increased TiO<sub>2</sub> content reduced the scorch time and cure time because TiO<sub>2</sub> is a metal oxide that acts as a co-activator, stimulating crosslinking during sulphur curing.

The cure time is the time it takes for the rubber to reach 90% of its final cure. The effect of titanium dioxide content is trivial to the cure time. It only shows a slight difference between one another. However, adding titanium dioxide slightly increases the cure time. The composite sample achieved the highest cure time at 0.3 wt% titanium dioxide. The composite requires a longer time to cure. The T<sub>90</sub> indicated the onset of the vulcanizing process was delayed. The delayed vulcanization behaviour increases the rubber's ability to withstand stress at large strains [12].

The torque difference (MH-ML) is a measure of dynamic shear modulus which indirectly relates to the crosslink density of the SiR composites [13]. The increasing interaction between TiO<sub>2</sub> and the SiR matrix can explain the increment of MH-ML values. This observation agrees with Alam *et al.*, [14] with work on thiuram-type accelerators. The researcher indicates that after reaching the lowest torque, it gradually increases, reaches a maximum value, and then is parallel or decreases with the vulcanization time. The decreasing torque after reaching the highest torque is called reversion. This condition might be due to the rubber's thermally unstable crosslink density degradation. In addition, the higher MH-ML values are represented by the higher crosslink density in the rubber. Incorporating titanium dioxide might increase the crosslink density compared to the control sample, except at the 0.3 and 0.6 wt% TiO<sub>2</sub>.

The CRI values of TiO<sub>2</sub>-reinforced samples are lower than the control sample. A smaller CRI indicates a faster cure rate. Nevertheless, the highest CRI value was achieved at SiR reinforced with 0.3 wt% TiO<sub>2</sub>. It shows that this sample experienced the slowest curing rate compared to other samples. This is due to the addition of titanium dioxide in the SiR composite samples, which increases the hydroxyl group levels and the vulcanization rate [15]. Thus, the crosslinking reaction was accelerated due to the hydroxyl group. However, 0.6 and 1.2 wt% TiO<sub>2</sub> showed lower CRI. As mentioned earlier, excessive TiO<sub>2</sub> added in SiR had a greater effect on reducing the scorch time. Chueangchayaphan *et al.*, [11] indicated that increased TiO<sub>2</sub> content reduced the scorch time and cure time because TiO<sub>2</sub> is a metal oxide that acts as a co-activator stimulating crosslinking during sulphur curing.

The hardness test evaluates a material's resistance to indentation or abrasion when subjected to contact with another material [16]. Table 2 tabulates the hardness of SiR and SiR composites with different percentages of titanium dioxide. Overall, the hardness results increased with the increased contents of TiO<sub>2</sub>, except at 1.2 wt% TiO<sub>2</sub>. The hardest was the SiR composite filled with 0.6 wt% TiO<sub>2</sub>. Meanwhile, the lowest hardness was SiR composite filled with 1.2 wt% TiO<sub>2</sub>. Hardness values agree with the maximum torque (MH) except for the sample at 1.2 wt% TiO<sub>2</sub>.

In general, increasing hard ceramic fillers in rubber matrix will increase the hardness value of the composites. Yet, the highest amount of titanium dioxide at 1.2 wt% exhibited the lowest hardness compared to other samples. This condition is due to porosity caused by trapped air bubbles in the samples. When the porosity increases, the hardness of the material will decrease [17]. Thus, pores or voids in a material diminish the volume of solid material, weakening the overall structure.

Adding an excessive amount of TiO<sub>2</sub> to rubber composites can form many pores due to the agglomeration of TiO<sub>2</sub> particles. When the concentration of TiO<sub>2</sub> is high, the particles tend to cluster together, forming agglomerates. These agglomerates create voids or pores in the rubber matrix. However, the sample at 0.6wt% TiO<sub>2</sub> has higher hardness due to the material containing better filler

dispersion and distribution, a smoother surface, and a lack of porosity. Hence, the sample at 0.6 wt% TiO<sub>2</sub> has higher hardness.

Overall, density depends on the structure, samples' mass and volume. In this case, TiO<sub>2</sub> of ~ 4.26 g/cm<sup>3</sup> has a higher density than silicon rubber of ~1.1 g/cm<sup>3</sup>. Therefore, including TiO<sub>2</sub> should have increased the overall sample density. In addition, density also depends on the filler's distribution and the presence of pores. Based on the graph, the highest density (1.07 g/cm<sup>3</sup>) was obtained by SiR reinforced with 0.6wt% TiO<sub>2</sub>. Meanwhile, the lowest density (0.873 g/cm<sup>3</sup>) was SiR composite with 1.2 wt% TiO<sub>2</sub>. This finding agrees with Colom *et al.*, [18] in their work. There is an inverse relationship between porosity and bulk density; as bulk density increases, porosity decreases. Hence, the higher the porosity, the lower the density.

### 3.2 Tensile Properties

The tensile strength of SiR reinforced with 0.3 wt% TiO<sub>2</sub> is the highest, as depicted in Figure 4(a). Hence, the sample is stronger and capable of withstanding higher tensile stress than other samples. However, adding excessive TiO<sub>2</sub> decreased the silicone rubber's tensile strength except at 0.3 wt% TiO<sub>2</sub>. The composite with 0.3 wt% TiO<sub>2</sub> has higher tensile strength. It might be the contribution of efficient crosslink density and good matrix-filler interaction in the SiR reinforced with 0.3wt% titanium dioxide sample. The observations agree with the MH-ML value, optimum cure time and the cure rate index.

Meanwhile, adding titanium dioxide of more than 0.3 wt% reduced tensile strength with strength value differences and wide standard deviations of 0.6 and 1.2 wt% TiO<sub>2</sub> samples, showing the contribution is trivial at this level. The wide deviation value reflects the inhomogeneity of the filler dispersion in the SiR matrix, as seen in the morphological analysis. The tensile strength of samples decreased as the contents of TiO<sub>2</sub> increased more than 0.3 wt%. The 0.6 wt% TiO<sub>2</sub> gave a dramatic drop in tensile strength once the content of TiO<sub>2</sub> increased. The tensile strength value at 0.6 wt% TiO<sub>2</sub> (0.70MPa) decreased by approximately 63 % compared to control samples at 0 wt% TiO<sub>2</sub> (1.11MPa). As mentioned in a study by Datta *et al.*, [7], demonstrated that adding five parts per hundred rubber (phr) of nano-TiO<sub>2</sub> improved mechanical properties. Consequently, a higher concentration of nano-TiO<sub>2</sub> particles resulted in a decrease in mechanical properties.

Figure 4(b) represents the elongation at break (EB) of SiR and SiR composites with different percentages of TiO<sub>2</sub>. The highest elongation at break was achieved by 0.3 wt% TiO<sub>2</sub> reinforced sample followed by 1.2, 0.0, and 0.6 wt%. The graphs also show that the EB decreased with a rise in the TiO<sub>2</sub> (more than 0.3wt%). It coincided with the modulus values where the 0.3wt% showed the lower M100, showing the high flexibility and stretchability of the sample.

Meanwhile, Figure 4(c) and Figure 4(d) depict the M100 and M300 values. The M100 and M300 are generally increased in all samples due to the stiffening of rubber chains under loading. However, the M300 values were absent or decreased in samples when they almost reached the point of breaking. All samples could be stretched to 100% elongation, but only several samples survived at 300% elongation. At M100, the control sample achieved the highest modulus (0wt% TiO<sub>2</sub>), and the lowest samples were at 0.6 wt% titanium dioxide. However, at M300, the sample at 0.6wt% and 1.2wt% TiO<sub>2</sub> experienced premature failure; therefore, no modulus value can be measured.

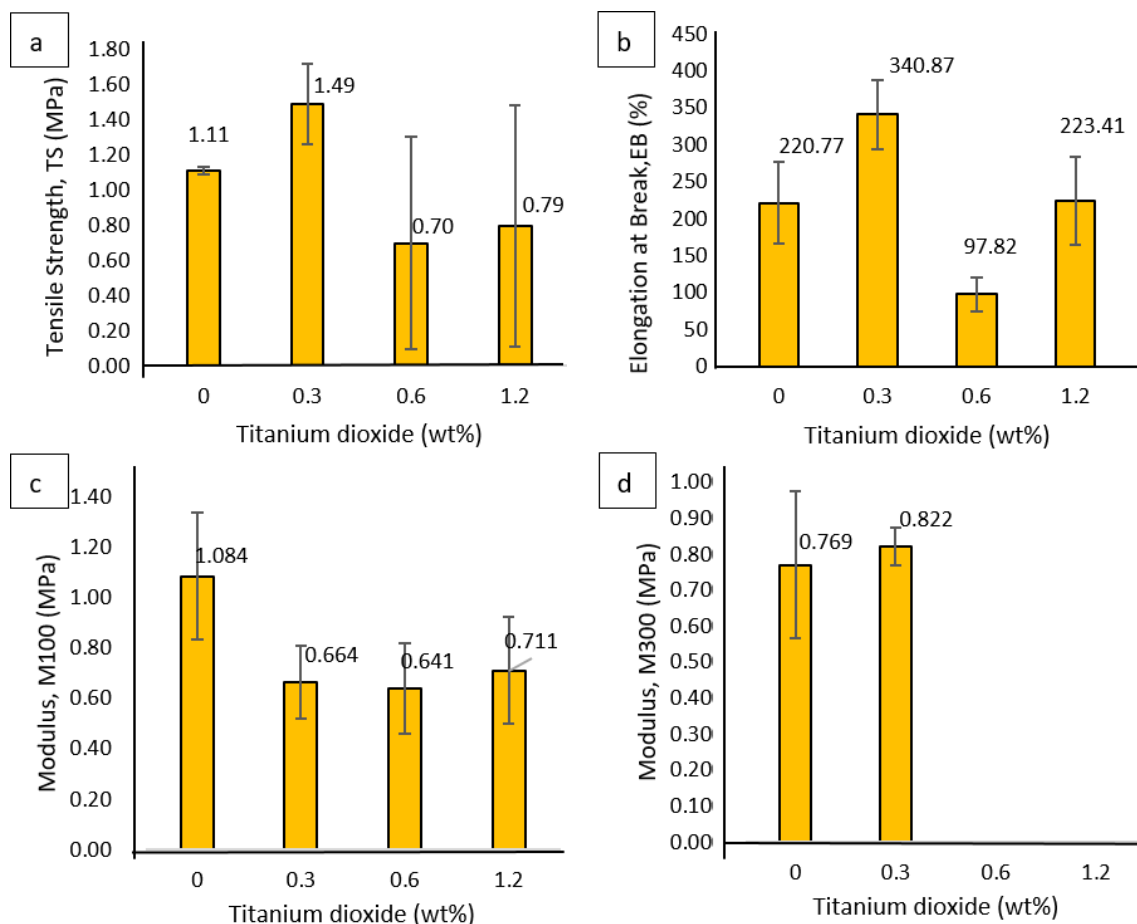


**Fig. 4.** (a) Tensile strength (TS), (b) Elongation at break (EB), (c) Modulus at 100% elongation (M100) and (d) Modulus at 300% elongation of silicone rubber composites at different percentages of titanium dioxide

This indication may be due to poorer matrix-filler interaction and less efficient crosslinking, which caused premature failure. It coincided with the increment of toluene uptakes by the samples in swelling analysis. In addition, the fracture surface changes from ductile to more brittle behaviour with an increase in the content of  $\text{TiO}_2$ , as discussed in SEM. The fracture surface of samples turned to smoothen, showing less shear yielding and tearing mechanisms, indicating less ductile fracture behaviour.

This finding agrees with Sim *et al.*, [8] work. They have reported that an increase in filler content was observed to boost the elongation at break initially. Subsequently, a decline was attributed to the interplay between rubber and filler interactions. The heightened filler concentration initially improved rubber-filler interaction, facilitating the effective transfer of applied stress in the rubber composite. However, with a further increase in filler concentration, filler-filler interaction became more prominent, diminishing the rubber-filler interaction and ultimately reducing the elongation at break.

### 3.3 Swelling Analysis

Figure 5(a) shows the swelling measurement of silicone rubber with different percentages of  $\text{TiO}_2$ . The small toluene particles can penetrate the rubber structures' opened structure and result in swelling. Samples with a more open structure will experience more swelling than samples with a more closed structure. In addition, the graph of swelling percentage and toluene uptake in Figure

5(b) shows an increment of toluene uptake with the percentage of  $\text{TiO}_2$ . There is good agreement with Kamarudin *et al.*, [19] on water absorption properties in silicone rubber studies. The researchers indicate that the lesser the porosity, the lower the water absorption percentages.

Based on Figure 3, the 1.2 wt%  $\text{TiO}_2$  absorption of a solvent (toluene) was the highest due to porous materials having more space in the form of voids or pores. When introduced, a solvent can fill these spaces, leading to an increase in the overall volume or mass of the material. The higher swelling percentage and toluene uptake represent lower crosslink density. It is widely accepted that the toluene uptake is directly correlated to the crosslink density of a network chain, whereby less solvent penetrates through the composites, indicating higher crosslink density [13]. Too high crosslink density is not always favorable as it can decrease the elongation at break, toughness and other functional properties of rubber composites. Therefore, efficient crosslink density is crucial in improving tensile strength and Young modulus.

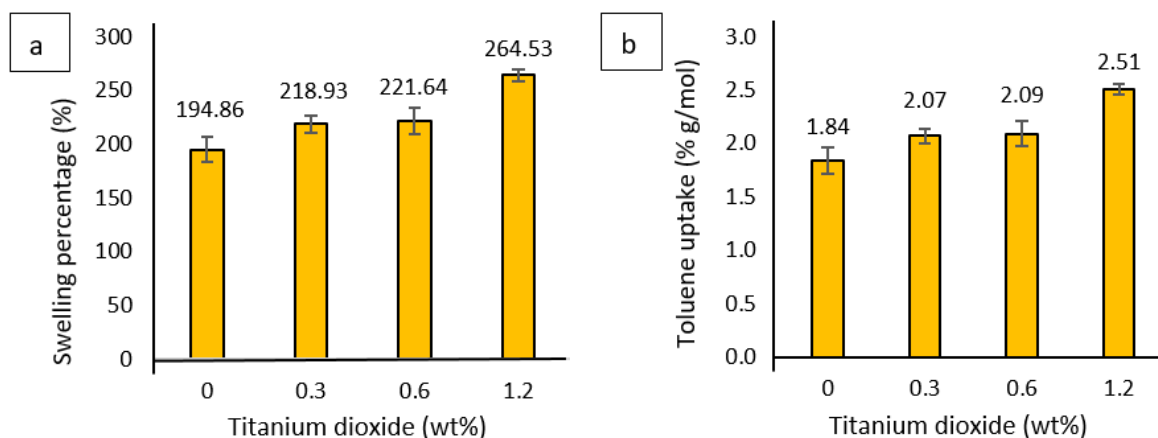


**Fig. 5.** (a) Swelling percentage of silicone rubber with different percentages of titanium dioxide and (b) Toluene uptake of silicone rubber with different percentages of titanium dioxide

### 3.4 Fourier Transform Infrared Spectroscopy (FTIR) Analysis

Figure 6 presents the infrared spectra of the composites. Major peaks for  $\text{TiO}_2$  occur at  $3497\text{ cm}^{-1}$  (O-H stretch),  $1630\text{ cm}^{-1}$  (Ti-OH bending), and  $483\text{ cm}^{-1}$  (Ti-O bending) [20,21]. The SiR composite reinforced with 0.3wt%  $\text{TiO}_2$  shows a sharp and strong Ti-O bending peak at  $483\text{ cm}^{-1}$ , correlating with its tensile strength and cure characteristics. SiR displays characteristic peaks at  $2962\text{ cm}^{-1}$  (C-H stretch in  $\text{CH}_3$ ),  $1257\text{ cm}^{-1}$  (Si- $\text{CH}_3$  deformation),  $1086$  to  $1007\text{ cm}^{-1}$  (Si-O-Si stretch), and  $791\text{ cm}^{-1}$  (Si-C stretch in Si-( $\text{CH}_3$ )<sub>2</sub>) [21,22]. Adding fillers does not significantly shift HTV-SiR's peaks, but hydrogen bonding between Si-O-Si (from HTV-SiR) and oxygen groups from  $\text{TiO}_2$  is observed. The FTIR analysis confirms the presence of hydroxyl groups on the composite surface, suggesting that a higher hydroxyl group count may enhance the composite's hydrophilic nature [7].

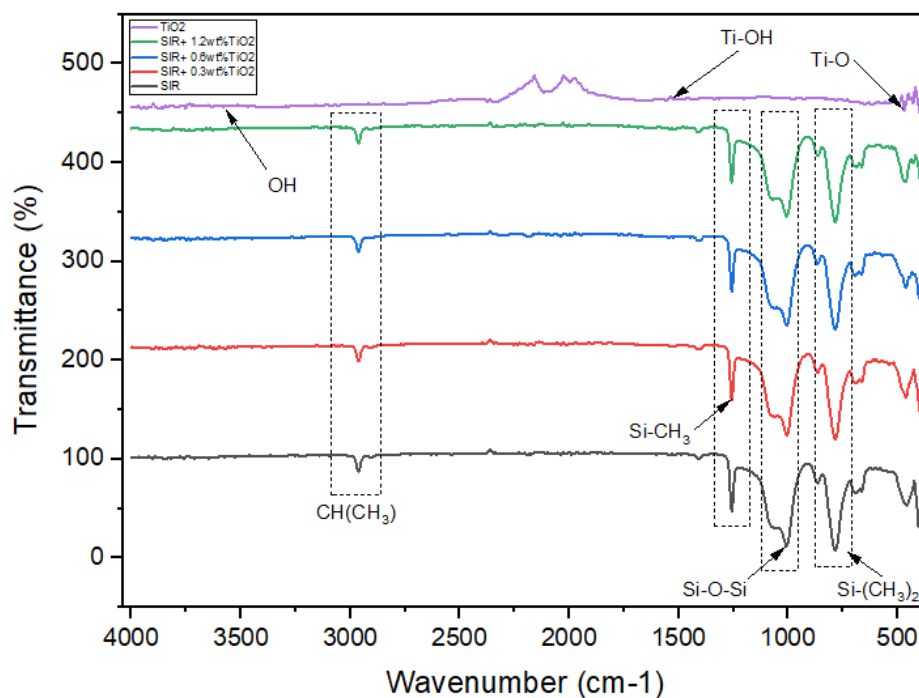


**Fig. 6.** FTIR spectra of HTV silicone rubber composites compare to virgin silicone rubber and titanium dioxide

### 3.5 X-ray Diffraction Spectroscopy (XRD)

The XRD spectra are shown in Figure 7. They reveal how the titanium dioxide affected the SiR composite's structural properties through the changes in the position and intensities of X-ray diffraction peaks [23]. The crystalline phase will appear as a sharp peak, but the amorphous phase may appear as a broadening peak.

The spectra show nearly identical peaks, with slight shifts to the left due to varying titanium dioxide content. A sharp reflection at  $2\theta = 34^\circ\text{--}37^\circ$  corresponds to the strongest silicon line of (111) orientation [24]. Excessive TiO<sub>2</sub> can interact with polymer chains and influence crystallization, altering the crystalline structure. The leftward shift of the (111) and (220) peaks suggests changes in crystal plane spacing or atom arrangement within the lattice, indicating TiO<sub>2</sub>'s impact on the crystallization process and crystalline region orientation in the silicone rubber. TiO<sub>2</sub> particles may also affect polymer chain packing, changing lattice parameters and the diffraction pattern.

Increasing the TiO<sub>2</sub> percentage may create smaller crystalline domains or alter intermolecular interactions, affecting crystal plane spacing. TiO<sub>2</sub> particles interacting with the silicone rubber matrix could cause material strain or stress, shifting the XRD peak position. Consequently, samples with 0.6 and 1.2 wt% TiO<sub>2</sub> exhibit lower tensile strength. An increase in the sharpness of the (102) peak in these samples suggests enhanced crystallinity in the silicone rubber's amorphous region due to TiO<sub>2</sub> diffusion between the rubber chains [25].

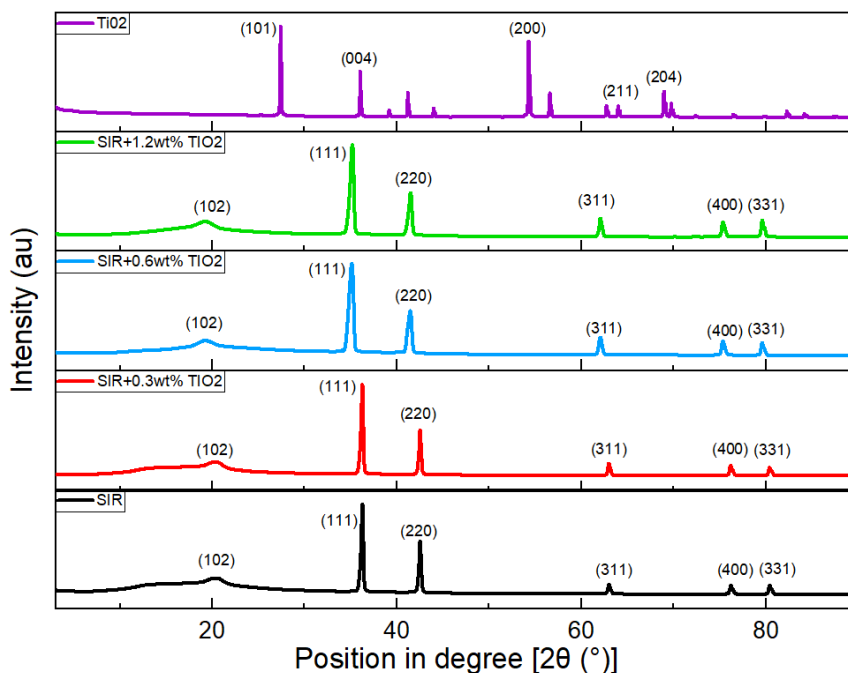


**Fig. 7.** XRD spectra of silicone rubber with different percentages of titanium dioxide

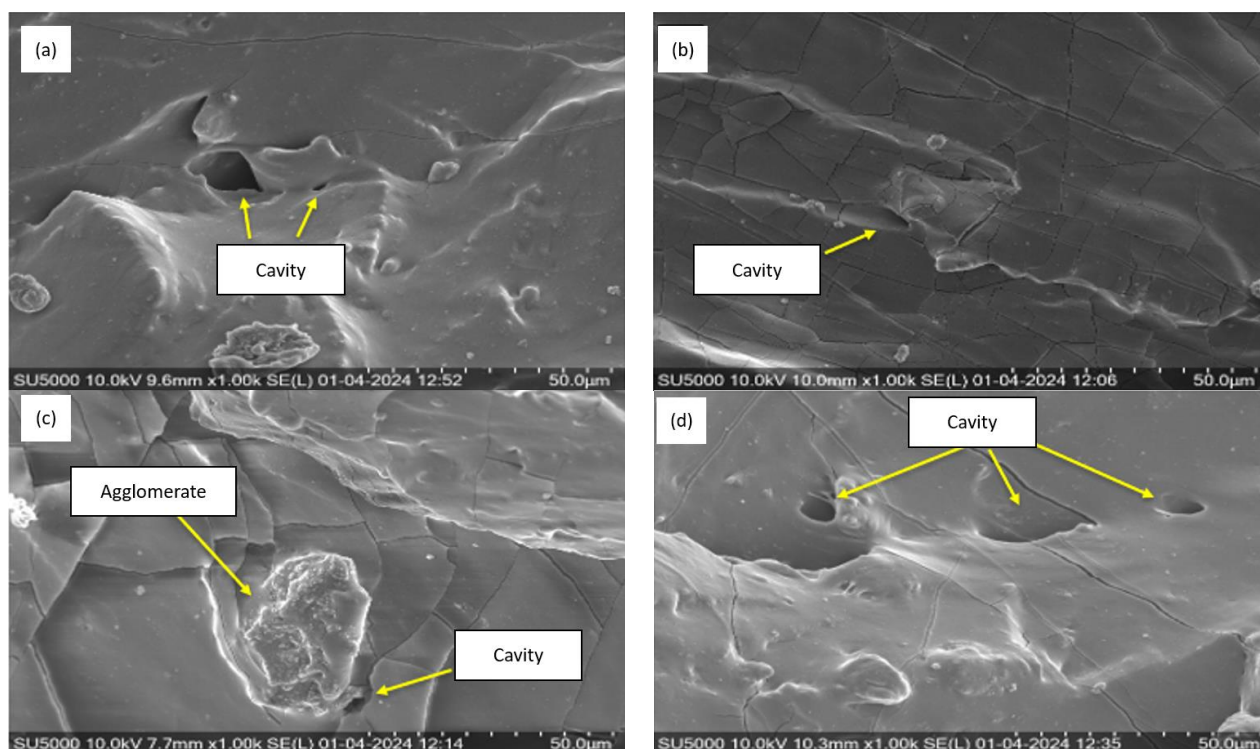
### 3.6 Scanning Electron Microscopy (SEM) Analysis

Figure 8 illustrates the SEM micrographs taken from the tensile fracture surfaces of (a)-moderate, (b)-best, (c)-worst and (d)-porosity at a magnification of 1000X. The dark phase represents the SiR matrix, and the bright phase corresponds to the titanium dioxide particles [26]. The micrographs reveal the fracture surfaces' morphology and structure and the filler particles' distribution and dispersion within the rubber matrix. There are microcracks on the surface due to the coating cracking during SEM. These microcracks are unrelated to the composites' mechanical properties and can be ignored. All samples showed the presence of cavities from the pull-out mechanism of fillers added in the rubber formulation.

Figure 8(a) and Figure 8(d) reveal significant filler pull-out, which manifested as cavities in samples with 0.0 and 1.2 wt% titanium dioxide, respectively, leading to the lowest tensile strength and elongation at break among the composites. This indicates that inappropriate concentrations of titanium dioxide can negatively impact the mechanical performance of silicone rubber composites. During mechanical loading, weakened or failed interfacial bonding can cause filler particles to detach, creating voids or cavities that reduce the effective cross-sectional area and increase stress concentration, leading to premature failure. These detached particles do not contribute to reinforcement and may initiate cracks. Consequently, samples with 0.0 and 1.2 wt%  $\text{TiO}_2$  exhibit poor interfacial adhesion and stress transfer, resulting in low tensile properties.

The silicone rubber composite with 0.3 wt%  $\text{TiO}_2$ , as shown in Figure 8(b), exhibits thinner tearing lines and smaller cavities, indicating the least agglomerates and filler pull-out, leading to the highest tensile strength and elongation at break [27]. This optimal concentration of  $\text{TiO}_2$  enhances the mechanical performance of the composites by promoting good interfacial adhesion, efficient stress transfer, and increased tensile properties. However, Figure 8(c) highlights the issue of filler agglomeration within the composite, which can initiate cracks under stress, compromise the material's structural integrity, and lead to premature failure [26]. Therefore, achieving uniform

nanofiller dispersion is crucial for optimizing the composite's mechanical performance, emphasizing the importance of proper dispersion techniques in manufacturing rubber composites.



**Fig. 8.** SEM micrographs showing tensile fracture surface of SiR and SiR composites reinforced with different percentages of titanium dioxide at 1000X magnifications: (a) 0.0 wt%; (b) 0.3 wt%; (c) 0.6 wt% and (d) 1.2 wt%

#### 4. Conclusions

The study investigated the effects of different concentrations of  $\text{TiO}_2$  nanofillers on the cure, mechanical, swelling, and structural properties of silicone rubber (SiR) composites. Based on the experimental results, the following conclusions can be drawn

- i. The optimal concentration of  $\text{TiO}_2$  for SiR composites was 0.3 wt%, which resulted in the highest tensile strength, modulus, elongation at break, and cure rate index among the four samples.
- ii. The addition of  $\text{TiO}_2$  increased the hardness and density of the SiR composites, except for the 1.2 wt%  $\text{TiO}_2$  composite, which had the highest porosity and swelling percentage due to filler agglomeration and poor dispersion.
- iii. The compositional, structural and morphological characteristics conform with the cure characteristics and physico-mechanical properties of the SiR and SiR composites.

Overall, the findings will be an outstanding contribution to the rubber industries in producing products with appreciable properties and microbial resistance.

#### Acknowledgement

Special acknowledgement to the Fakulti Teknologi Kejuruteraan Industri dan Pembuatan, Universiti Teknikal Malaysia Melaka (UTeM) and Rubber Leisure Products Sdn Bhd for providing the resources and facilities for the research. This research was not funded by any grant.

## References

- [1] Alarifi, Ibrahim M. "A comprehensive review on advancements of elastomers for engineering applications." *Advanced Industrial and Engineering Polymer Research* 6, no. 4 (2023): 451-464. <https://doi.org/10.1016/j.aiepr.2023.05.001>
- [2] Ghamrawi, Sarah, Jean-Philippe Bouchara, Alexandre Corbin, Sergiy Rogalsky, Oksana Tarasyuk, and Jean-François Bardeau. "Inhibition of fungal growth by silicones modified with cationic biocides." *Materials Today Communications* 22 (2020): 100716. <https://doi.org/10.1016/j.mtcomm.2019.100716>
- [3] Montazer, Zahra, Mohammad B. Habibi Najafi, and David B. Levin. "Challenges with verifying microbial degradation of polyethylene." *Polymers* 12, no. 1 (2020): 123. <https://doi.org/10.3390/polym12010123>
- [4] Celina, Mathew C. "Review of polymer oxidation and its relationship with materials performance and lifetime prediction." *Polymer Degradation and Stability* 98, no. 12 (2013): 2419-2429. <https://doi.org/10.1016/j.polymdegradstab.2013.06.024>
- [5] Kashi, Sima, Russell Varley, Mandy De Souza, Salwan Al-Assafi, Adriano Di Pietro, Christelle de Lavigne, and Bronwyn Fox. "Mechanical, thermal, and morphological behavior of silicone rubber during accelerated aging." *Polymer-Plastics Technology and Engineering* 57, no. 16 (2018): 1687-1696. <https://doi.org/10.1080/03602559.2017.1419487>
- [6] Aysa, Noor Hadi, Mohamed Hamza Al-Maamori, and Nehad Abdul Ameer Al-Maamori. "Effect of the unmodified and modified ZnO nanoparticles on the mechanical and antibacterial properties of silicone rubber using in medical applications." *Journal of Nanoscience and Nanoengineering* 1, no. 3 (2015): 119-124.
- [7] Datta, Janusz, Paulina Kosiorok, and Marcin Włoch. "Effect of high loading of titanium dioxide particles on the morphology, mechanical and thermo-mechanical properties of the natural rubber-based composites." *Iranian Polymer Journal* 25 (2016): 1021-1035. <https://doi.org/10.1007/s13726-016-0488-7>
- [8] Sim, L. C., C. K. Lee, S. R. Ramanan, H. Ismail, and K. N. Seetharamu. "Cure characteristics, mechanical and thermal properties of Al<sub>2</sub>O<sub>3</sub> and ZnO reinforced silicone rubber." *Polymer-Plastics Technology and Engineering* 45, no. 3 (2006): 301-307. <https://doi.org/10.1080/03602550500373683>
- [9] Wu, Jian, Jiye Dong, Youshan Wang, and Bipin Kumar Gond. "Thermal oxidation ageing effects on silicone rubber sealing performance." *Polymer Degradation and Stability* 135 (2017): 43-53. <https://doi.org/10.1016/j.polymdegradstab.2016.11.017>
- [10] Mohamad, N., A. Muchtar, M. J. Ghazali, H. M. Dahlan, and C. H. Azhari. "Epoxidised natural rubber-alumina nanoparticle composites (ENRAN): effect of filler loading on the tensile properties." *Solid State Science and Technology* 17, no. 2 (2009): 133-143.
- [11] Chueangchayaphan, Wannarat, Piyawadee Luangchuang, and Narong Chueangchayaphan. "High Performance of Titanium Dioxide Reinforced Acrylonitrile Butadiene Rubber Composites." *Polymers* 14, no. 23 (2022): 5267. <https://doi.org/10.3390/polym14235267>
- [12] Yan, Zhu, Ali Zaoui, and Fahmi Zaïri. "Physical and mechanical properties of vulcanized and filled rubber at high strain rate." *Chinese Journal of Physics* 86 (2023): 12-23. <https://doi.org/10.1016/j.cjph.2023.09.010>
- [13] Hong, Choy Jun, Noraiham Mohamad, Hairul Effendy Ab Maulod, Jeefferie Abd Razak, Toibah Abd Rahim, Mohd Sharin Ghani, Nor Hidayah Rahim, Soh Tiak Chuan, Dewi Suriyani Che Halin, and Mohammed Iqbal Shueb. "Crosslink Density and Toluene Sorption of Tin Dioxide Reinforced Deproteinized Natural Rubber Nanocomposites." *Journal of Advanced Research in Applied Mechanics* 111, no. 1 (2023): 103-119. <https://doi.org/10.37934/aram.111.1.103119>
- [14] Alam, Md Najib, Vineet Kumar, Pranot Potiyaraj, Dong-Joo Lee, and Jungwook Choi. "Synergistic activities of binary accelerators in presence of magnesium oxide as a cure activator in the vulcanization of natural rubber." *Journal of Elastomers & Plastics* 54, no. 1 (2022): 123-144. <https://doi.org/10.1177/00952443211020794>
- [15] Nor, N. A. Mohd, and N. Othman. "Effect of filler loading on curing characteristic and tensile properties of palygorskite natural rubber nanocomposites." *Procedia Chemistry* 19 (2016): 351-358. <https://doi.org/10.1016/j.proche.2016.03.023>
- [16] Subramani, Karthikeyan, and Waqar Ahmed, eds. *Emerging nanotechnologies in dentistry*. Elsevier, 2018. <https://doi.org/10.1016/c2016-0-00131-6>
- [17] Sampath, Wickramage Don Manjula, Shantha Maduwage Egodage, and Dilhara Githanjali Edirisinghe. "Effect of peroxide loading on properties of natural rubber and low-density polyethylene composites." *Journal of Physical Science* 30, no. 3 (2019): 49-69. <https://doi.org/10.21315/jps2019.30.3.4>
- [18] Colom, X., J. Girbau, M. Marin, Krzysztof Formela, Mohammad Reza Saeb, F. Carrillo, and J. Cañavate. "New approach in the reuse of modified ground tire rubber as thermal and acoustic insulation to be used in civil engineering." *Journal of Material Cycles and Waste Management* 25, no. 6 (2023): 3557-3566. <https://doi.org/10.1007/s10163-023-01778-6>

- [19] Kamarudin, Najwa, Jeefferie Abd Razak, Nurbahirah Norddin, Noraiham Mohamad, Lau Kok Tee, Tony Chew, and Nurzallia Mohd Saad. "Hardness and water absorption properties of silicone rubber based composites for high voltage insulator applications." In *Intelligent Manufacturing and Mechatronics: Proceedings of the 2nd Symposium on Intelligent Manufacturing and Mechatronics-SympoSIMM 2019*, 8 July 2019, Melaka, Malaysia, pp. 343-352. Springer Singapore, 2020. [https://doi.org/10.1007/978-981-13-9539-0\\_34](https://doi.org/10.1007/978-981-13-9539-0_34)
- [20] Chougala, L. S., M. S. Yatnatti, R. K. Linganagoudar, R. R. Kamble, and J. S. Kadadevarmath. "A simple approach on synthesis of TiO<sub>2</sub> nanoparticles and its application in dye sensitized solar cells." *Journal of Nano-and Electronic Physics* 9, no. 4 (2017): 4005-1.
- [21] Kumar, Vineet, Anuj Kumar, Minseok Song, Dong-Joo Lee, Sung-Soo Han, and Sang-Shin Park. "Properties of silicone rubber-based composites reinforced with few-layer graphene and iron oxide or titanium dioxide." *Polymers* 13, no. 10 (2021): 1550. <https://doi.org/10.3390/polym13101550>
- [22] Wang, Zhigao, Xinghai Zhang, Fangqiang Wang, Xinsheng Lan, and Yiqian Zhou. "Effects of aging on the structural, mechanical, and thermal properties of the silicone rubber current transformer insulation bushing for a 500 kV substation." *SpringerPlus* 5, no. 1 (2016): 790. <https://doi.org/10.1186/s40064-016-2549-y>
- [23] Pecharsky, Vitalij K., and Peter Y. Zavalij. *Fundamentals of powder diffraction and structural characterization of materials*. Springer US, 2009. <https://doi.org/10.1007/978-0-387-09579-0>
- [24] Westra, J. M., V. Vavruřková, P. Šutta, R. A. C. M. M. Van Swaij, and M. Zeman. "Formation of thin-film crystalline silicon on glass observed by in-situ XRD." *Energy Procedia* 2, no. 1 (2010): 235-241. <https://doi.org/10.1016/j.egypro.2010.07.034>
- [25] Shamsudin, Zurina, Adibah Haneem Mohamad Dom, Muhammad Afiq A. Razak, Maturah Mesri, and Mulyadi Mulyadi. "Analysis on the Effect of Elevated Loading of Reclaimed Spent Bleach Earth on Physico-Mechanical Properties of PLA Polymer Composite in Single Screw Extrusion Process." *Journal of Advanced Research in Applied Mechanics* 112, no. 1 (2024): 162-174. <https://doi.org/10.37934/aram.112.1.162174>
- [26] Rahim, N. H., K. Y. Lau, N. A. Muhamad, N. Mohamad, W. A. W. A. Rahman, and A. S. Vaughan. "Effects of filler calcination on structure and dielectric properties of polyethylene/silica nanocomposites." *IEEE Transactions on Dielectrics and Electrical Insulation* 26, no. 1 (2019): 284-291. <https://doi.org/10.1109/TDEI.2018.007796>
- [27] Ab Maulod, Hairul Effendy, Noraiham Mohamad, Jeefferie Abd Razak, Ahmad Aqlan Mohd Rosedi, Andri Andriyana, Nurzallia Mohd Saad, and Moayad Husein Flaifel. "Effect of Different Waste Coal Ash (WCA) Loading to Dynamic Load Application of Chloroprene Rubber." *Malaysian Journal on Composites Science and Manufacturing* 3, no. 1 (2020): 27-37. <https://doi.org/10.37934/mjcs.3.1.2737>